A Study on the Effects of Wave Spectra on Wave Energy Conversions

James Prendergast, Mingfang Li, and Wanan Sheng

***Abstract*—This research work presents an investigation into the effects of wave spectra on energy conversion for wave energy converters and shows it may be important what theoretical spectrum should be used for a better assessment of a wave energy converter (WEC) in the given sea conditions in a proposed deployment site. To illustrate the problem and the solution, a slightly modified Reference Model 3 (RM3) self-referencing floating point absorber device is used for examining the effects of spectrum types on wave energy conversion. The compared wave spectra include the most used theoretical wave spectra, such as the standard JONSWAP and Bretschneider spectra, as well as the real sea spectrum from field measurements. From the analysis it is shown that the modified RM3 WEC extracts a similar amount of energy from the recorded sea conditions (measured at the AMETS site 2010) when the device is optimized to both the Bretschneider spectrum and the real sea spectrum while the use of the JONSWAP spectrum for optimization leads to an over-prediction in the annual energy production of 16.5%. This may be because, in many practical applications for wave energy development, the JONSWAP spectrum is often preferred by the developers for assessing the device power performance. However, the use of the narrower JONSWAP spectrum (compared to the Bretschneider spectrum) may lead to inaccurate optimization results and power performance data for the device. Therefore, using the correct wave spectrum shapes in the assessment and optimization of a device is suggested for a more accurate assessment and a better understanding of the overall power performance of the device.**

***Index Terms*—Annual energy production (AEP), optimization, power performance, wave climate, wave energy conversion.**

Manuscript received May 10, 2018; revised July 20, 2018 and August 30, 2018; accepted September 6, 2018. The work of M. Li was supported in part by the China Scholarship Council (CSC 201608420160) during a visit to University College Cork, in part by the Research Project of Hubei Provincial Department of Education (Q20171110), and in part by the Hubei Province Key Laboratory of Systems Science in Metallurgical Process (Wuhan University of Science and Technology, Z201503). The work of W. Sheng was supported in part by the Science Foundation Ireland, in part by the Centre for Marine and Renewable Energy Research under Grant 12/RC/2302, and in part by the Environmental Research Institute, University College Cork. *(Corresponding author: Mingfang Li.)*

Associate Editor: K. Takagi.

J. Prendergast is with the Energy Engineering, School of Engineering, University College Cork, Cork T12 K8AF, Ireland (e-mail: 116222268@umail.ucc.ie).

M. Li is with the Department of Mechanical Engineering, College of Science, Wuhan University of Science and Technology, Wuhan 430081, China (e-mail: limingfang@wust.edu.cn).

W. Sheng is with the MaREI Centre, Environmental Research Institute, University College Cork, Cork T12 K8AF, Ireland (e-mail: wanan_sheng@outlook.com).

Digital Object Identifier 10.1109/JOE.2018.2869636

I. Introduction

With the signing of the Paris Agreement and the ambition for the European Union to have a carbon free energy system by 2050, a greater emphasis and importance has been placed on renewable energy technologies [1]. Ocean energy represents one of the largest untapped renewable energy resources with the vast available resources and the wide distribution around the globe [2]. Currently, ocean energy technologies, especially the wave energy technologies, are not matured enough yet for commercial energy generation, but it is hoped that they will become significant suppliers in the future energy mix when the main technological and nontechnological issues are resolved, such as finance, technology development, environmental issues, and grid connections [3].

Ireland, in particular, stands to benefit significantly from the development of ocean energy. This is apparent from the number of companies based in Ireland that develop ocean energy converters, such as OpenHydro [4], OceanEnergy, Ltd., [5], and SeaPower [6], among others. According to the Sustainable Energy Authority of Ireland, Dublin, Ireland, report carried out by ESBI (ESB International, owned by the Electricity Supply Board, Ireland), Ireland has a theoretical wave energy resource of up to 525 TWh [7], which is significantly more than the electricity consumed in Ireland in 2015 (26.98 TWh according to an IEA report from 2015). The harnessing of this vast resource would greatly improve Ireland's energy security as currently its energy system is heavily reliant on imported gas and coal to fire its thermal generation stations, allowing for the phasing out the aforementioned thermal generation stations, reducing energy costs, and CO_2 emissions. The significant wave energy potential could also benefit Ireland economically with the current and planned interconnection allowing for the sale of energy to foreign markets.

Wave energy technologies are still in development, and many different types of wave energy converters have been proposed, but only few have been advanced to higher technology readiness levels. Examples of these technologies include the LIMPET [8], Pelamis [9], Oyster [10], OPT [11], WaveDragon [12], WaveStar [13] and more recently, CorPower [14], and Floating Power Plant [15].

An important issue is the reliable and accurate assessment of the device to its given wave climate and based on that the relevant optimization to the device and the power takeoff (PTO) setting can be carried out for efficiently extracting wave energy, thus improving the cost effectiveness of the device in wave

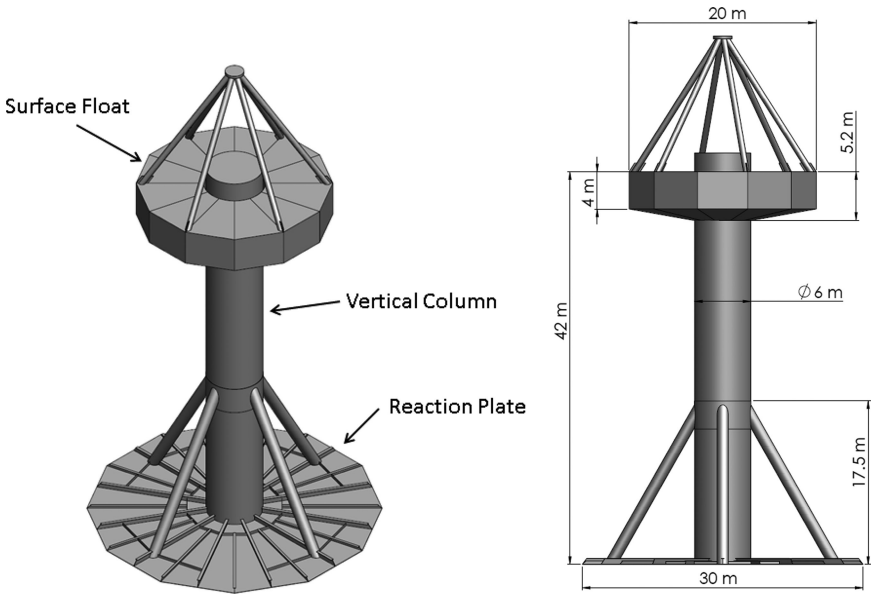

Fig. 1. RM3 device and the dimension [19].

energy production. Historically, such an assessment may be simply conducted using the theoretical wave spectra, such as the standardized JONSWAP and Bretschneider spectra, in particular the JONSWAP spectrum may be the most popular one chosen by the device developers. However, using different spectra may lead to very different results in the power conversion assessment, since these two theoretical spectra have different bandwidths, which is frequently an important factor in energy conversion of the wave energy converters.

The aim of this research work is to investigate the effects of wave spectra on the energy conversion of wave energy converters. To achieve this, the following information was used.

1) The wave energy converter chosen for the investigation is the reference model 3 (RM3, USA [16]), a self-referencing floating point absorber (PA) type WEC, with a slight modification for the wave climate used for the research work.
2) The energy extraction from sea waves/spectra uses the method given in [17], in which the max wave energy conversion has been achieved by optimizing the PTO.
3) The wave climate is considered from the wave measurements at the Atlantic Marine Energy Test Site in 2010 (AMETS, Ireland).
4) Three different types of wave spectra: Bretschneider, JONSWAP, and the measured spectra, will be used for assessing the device's power performance and comparison.
5) For a fair comparison, the rated power of the device is taken as 800 kW. Based on the assumptions and conditions outlined above, we analyzed the power performance of RM3 device using Bretschneider, JONSWAP, and the measured spectra to illustrate a more accurate theory spectra choice.

The rest of this paper consists of the following sections. Section II introduces briefly the RM3 wave energy converter and the modification adopted in the research; the analysis method including the PTO optimization is given in Section III; in Section IV, the power performance is given using the power matrices, while in Section V a further analysis and comparison is given. Finally, the conclusions are given in Section VI.

II. RM3 Device

The RM3 is a self-referencing floating PA type WEC developed as part of the Reference Model Project [18] (see Fig. 1). The Reference Model Project was established with two key aims, to design and develop several ocean energy harvesting devices to gauge the readiness of these technologies for commercial applications and to identify the areas where further research and development could be best applied to advance development and make the technologies ready for commercial use [19].

Although the RM3 uses a hydraulic PTO system located in the vertical column of the device to harness the power in the real sea waves, the maximized power for such a device can still be modeled using a linear PTO (see [17]). This allows for the dynamics and power conversion of the device to be modeled in the frequency domain, and avoids the need for using time-domain modeling that proves time consuming.

To ensure a better assessment of the power extraction from seas it is imperative that the device and PTO should be optimized for the conditions similar or close to the measured sea states.

As was mentioned earlier the device is modified for the AMETS wave conditions, a 27.5 m heave plate is used to replace the standard 30 m heave plate as it was found that the device had a higher coefficient of power in the conditions used in this study (see [20]). For the modified RM3 design (D = 27.5 m), the float has a heave resonance period of 5.37 s, but the spar has a heave resonance of 33.07 s [see Fig. 2 (left)]. Apparently, these two heave resonance periods cover a large range of the waves.

Fig. 2 (right) shows the maximal capture powers for the modified RM3 PA. There is a gain for the PA over a range of wave

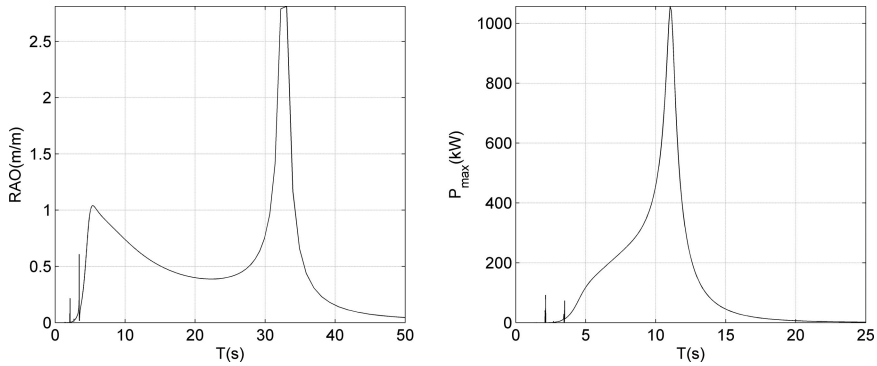

Fig. 2. Relative heave RAOs and maximal capture powers in regular waves for the RM3 (self-referenced, heave plate D = 27.5 m) [20].

periods. For the case of D = 27.5 m, the gain is for the periods from 6.5 to 12.5 s, which just falls on the wave periods of interest based on common wave energy resource assessment. For the self-referenced PA, there is large but narrow peaks at T = 11 s, which may be responsible for the capture power increase for the self-referenced PA.

III. Analysis Method

This section details the methods used to carry out the research. The techniques, assumptions, and equations used throughout the research project will be outlined and, if required, explained in a clear and concise manner. A step by step guide on the processes and methods used in the various stages of the project will be presented in a manner allowing for the application of the work carried out.

Section III-A details the steps taken to carry out the wave resource assessment of the recorded data, and the end result is a wave occurrence scatter diagram detailing the various sea states in the given location in a statistical manner, i.e., the wave climate. Section III-B details the calculation of the individual power matrices for each spectrum including the configuration of the RM3 device, damping, and power conversion. The calculation methods for each scenario vary slightly, but this will be shown in the individual sections.

A. Wave Climate

An accurate wave resource assessment is an important factor required for any successful wave power generation development. It is of particular importance to this study as the aim is to assess and optimize the device to the given wave conditions at the site, to ensure better power extraction. While wave energy resource assessments can be carried out and presented in many ways, the assessment carried out in this body of work aimed at producing a scatter diagram detailing the occurrence of the various wave conditions on the site. This method allows for the easy identification of the most prominent conditions as well as the largest waves the wave energy converters must survive.

The methods used in this study are based on the methods used by Sheng and Lewis [20] and Cahill and Lewis [21] throughout their studies. A bivariate analysis on the spectral data measured at the AMETS to determine the different occurrences of significant wave height and energy periods. The data used was recorded at the AMETS site in 2010 (the whole year) using two data recording buoys positioned in the 50 m deep water berth, with an overall availability of 75.28%.

To calculate the significant wave heights, H_s, and energy periods, T_e, from the 13 189 spectral measurements, it was first required to calculate the moments. The moments of a spectrum can be used to calculate various different wave statistics; however, in this case the methods for calculating H_s and the various wave statistic/characteristic periods are presented as follows:

$$H_s = 4\sqrt{m_0} \tag{1}$$

$$T_e = 2\pi \frac{m_{-1}}{m_0} \tag{2}$$

$$T_{01} = 2\pi \frac{m_0}{m_1} \tag{3}$$

$$T_{02} = 2\pi \sqrt{\frac{m_0}{m_2}} \tag{4}$$

with the *n*th-order moment being given as

$$m_n = \int_0^\infty S(\omega)\omega^n \, d\omega \tag{5}$$

where *n* = –2, –1, 0, 1, 2, depending on which moment you are calculating; *S*(ω) is the spectral value, and ω is the frequency.

Once the values for H_s and T_e were calculated for each sea state, the bivariate analysis is then carried out to determine the occurrence of different wave conditions measured. A bivariate scatter plot can be generated by grouping the significant wave heights and energy periods into different bins with the bins for significant wave height grouped from 0.25 to 14.25 m using a bin size of 0.5 m while the bins for the energy period measure from 4.25 to 14.25 s using a bin size of 0.5 s also (see Fig. 3). It can be seen that waves with an energy period in the range of 6 to 12.5 s have been found to be of the most happened waves, and thus of the most interest for wave energy conversion purposes [22].

B. PTO Optimization

1) PTO Optimization for Regular Waves: The analysis carried out follows the same methods as those in [17] and [20], but for completeness, a short introduction is given here.

Occurrence (%)	Energy period, Te (s)																				
Significant wave height, Hs (m)	4.25	4.75	5.25	5.75	6.25	6.75	7.25	7.75	8.25	8.75	9.25	9.75	10.25	10.75	11.25	11.75	12.25	12.75	13.25	13.75	14.25
14.25	0	0	0	0	0	0	0	0	0	0	0	0	0	0	0	0	0	0	0	0	0
13.75	0	0	0	0	0	0	0	0	0	0	0	0	0	0	0	0	0	0	0	0	0
13.25	0	0	0	0	0	0	0	0	0	0	0	0	0	0	0	0	0	0	0	0	0.01
12.75	0	0	0	0	0	0	0	0	0	0	0	0	0	0	0	0	0	0	0	0.02	0
12.25	0	0	0	0	0	0	0	0	0	0	0	0	0	0	0	0	0	0	0	0	0
11.75	0	0	0	0	0	0	0	0	0	0	0	0	0	0	0	0	0	0	0.01	0	0
11.25	0	0	0	0	0	0	0	0	0	0	0	0	0	0	0	0	0	0.01	0	0	0
10.75	0	0	0	0	0	0	0	0	0	0	0	0	0	0	0	0	0	0.01	0.02	0.01	0
10.25	0	0	0	0	0	0	0	0	0	0	0	0	0	0	0	0	0	0	0	0	0
9.75	0	0	0	0	0	0	0	0	0	0	0	0	0	0	0	0	0.02	0.03	0	0	0
9.25	0	0	0	0	0	0	0	0	0	0	0	0	0	0	0	0	0.03	0.01	0	0	0.02
8.75	0	0	0	0	0	0	0	0	0	0	0	0	0	0	0	0.01	0.02	0	0.01	0.01	0.02
8.25	0	0	0	0	0	0	0	0	0	0	0	0	0	0	0.01	0.02	0	0.02	0.03	0.01	0.01
7.75	0	0	0	0	0	0	0	0	0	0	0	0	0.01	0	0	0.02	0.03	0.05	0.01	0.01	0
7.25	0	0	0	0	0	0	0	0	0	0	0	0	0	0	0.02	0.02	0.05	0.05	0.02	0	0.01
6.75	0	0	0	0	0	0	0	0	0	0	0	0	0	0.02	0.04	0.09	0.09	0.06	0.02	0.01	0.01
6.25	0	0	0	0	0	0	0	0	0	0	0.01	0	0.04	0.09	0.13	0.11	0.09	0.01	0.02	0.02	0.01
5.75	0	0	0	0	0	0	0	0	0	0	0.02	0.02	0.07	0.14	0.14	0.12	0.03	0.02	0.02	0	0
5.25	0	0	0	0	0	0	0	0	0	0.02	0.07	0.14	0.24	0.21	0.14	0.11	0.03	0.02	0	0	0
4.75	0	0	0	0	0	0	0	0	0.06	0.11	0.28	0.34	0.35	0.31	0.22	0.14	0.05	0.02	0	0	0
4.25	0	0	0	0	0	0	0.01	0.08	0.12	0.52	0.6	0.72	0.47	0.27	0.2	0.12	0.08	0	0	0	0
3.75	0	0	0	0	0	0	0.04	0.16	0.5	0.83	0.95	0.86	0.55	0.52	0.37	0.1	0.03	0	0.05	0.01	0.01
3.25	0	0	0	0	0	0.07	0.11	0.51	0.89	1.49	2.06	1.57	1.05	0.68	0.51	0.34	0.1	0.08	0.05	0	0
2.75	0	0	0	0	0.09	0.21	0.74	1.15	2.14	2.61	2.58	1.58	1.15	0.9	0.56	0.39	0.26	0.09	0.1	0.02	0.01
2.25	0	0	0.01	0.02	0.17	0.57	1.71	2.03	2.15	2.42	1.87	1.53	1.18	0.68	0.36	0.21	0.14	0.15	0.13	0.09	0.03
1.75	0	0	0.11	0.67	1.08	1.74	1.93	2.81	3.43	3.71	2.68	1.79	1.15	0.49	0.2	0.17	0.1	0.03	0.02	0	0.01
1.25	0	0.02	0.46	1.34	0.92	1.5	2.18	2.38	3.1	2.24	2.28	1.74	1.02	0.55	0.2	0.03	0.05	0.05	0	0	0
0.75	0	0.09	0.14	0.55	0.3	0.71	0.95	0.79	0.49	0.33	0.4	0.14	0.06	0.03	0.02	0	0.01	0	0	0	0
0.25	0	0	0	0	0	0	0	0	0.01	0	0	0	0	0	0	0	0	0	0	0	0

Fig. 3. Wave scatter plot showing the wave occurrence for the AMETS site in 2010.

For the hydrodynamic analysis, potential flow theory is used as the basis for the boundary element method. In the analysis each of the two bodies of the device has six degrees of freedom, with the first body of the device, the spar, and the heave plate, being identified by the motion modes 1 to 6, representing its surge, sway, heave, roll, pitch, and yaw motions, respectively, and the second body of the device, the torus or float, identified by motion modes 7 to 12. In the wave energy conversion, the most important motions in this floating WEC are the relative heave motions of the two bodies. With a linear PTO, the dynamic equation is given in frequency domain as follows:

$$\begin{cases} \left[i\omega Q_{33} + b_{33} + B_{33}\right] v_3 + \left[i\omega Q_{39} + b_{39}\right] v_9 \\ \qquad = f_3 - B_{\text{pto}}(v_3 - v_9) \\ \left[i\omega Q_{93} + b_{93}\right] v_3 + \left[i\omega Q_{99} + b_{99} + B_{99}\right] v_9 \\ \qquad = f_9 + B_{\text{pto}}(v_3 - v_9) \end{cases} \tag{6}$$

with

$$\begin{cases} Q_{33} = (m_{33} + a_{33}) - \dfrac{c_{33}}{\omega^2}; Q_{39} = a_{39} - \dfrac{c_{39}}{\omega^2} \\ Q_{93} = a_{93} - \dfrac{c_{93}}{\omega^2}; Q_{99} = (m_{99} + a_{99}) - \dfrac{c_{99}}{\omega^2} \end{cases} \tag{7}$$

where B_{pto} is the damping coefficient of the PTO for the RM3 device; b_{33}, b_{39}, b_{93}, and b_{99} are the radiation damping coefficients due to the body motions; B_{33} and B_{99} are the additional linear damping coefficients caused by the heave motion of the bodies; f_3 and f_9 are the complex excitations for the heave motions of both moving bodies of the device; v_3 and v_9 are the velocities of the heave motions; m_{33} and m_{99} are the mass of each body; a_{33}, a_{39}, a_{93}, and a_{99} are the self- and cross-term added masses related to the heave motion of two bodies; and c_{33}, c_{39}, c_{93}, and c_{99} are the corresponding restoring force coefficients for the device.

The average power conversion is then given as follows:

$$\bar{P} = \frac{1}{2} B_{\text{pto}} |v_9 - v_3|^2 \tag{8}$$

with the relative velocity solved from (6), the average power is

$$\bar{P} = \frac{1}{2} B_{\text{pto}} \frac{Z_1^2 + Z_2^2}{(Y_1 + Y_2 B_{\text{pto}})^2 + \omega^2 (Y_3 + Y_4 B_{\text{pto}})^2}. \tag{9}$$

In the above-mentioned equation, Y_1, Y_2, Y_3, and Y_4 are the reactance-dependent damping coefficients and Z_1 and Z_2 are radiation damping and excitation-based values that are calculated as follows:

$$\begin{cases} Z_1 = f_{3r}\left(b_{99} + B_{99} + b_{93}\right) - f_{9r}\left(b_{33} + B_{33} + b_{39}\right) \\ \qquad -\omega f_{3i}\left(Q_{99} + Q_{93}\right) + \omega f_{9i}\left(Q_{33} + Q_{39}\right) \\ Z_2 = f_{3i}\left(b_{99} + B_{99} + b_{93}\right) - f_{9i}\left(b_{33} + B_{33} + b_{39}\right) \\ \qquad +\omega f_{3r}\left(Q_{99} + Q_{93}\right) - \omega f_{9r}\left(Q_{33} + Q_{39}\right) \\ Y_1 = \left(b_{33} + B_{33}\right)\left(b_{99} + B_{99}\right) - b_{93} b_{39} \\ \qquad -\omega^2\left(Q_{33} Q_{99} - Q_{93} Q_{39}\right) \\ Y_2 = b_{33} + B_{33} + b_{99} + B_{99} + b_{39} + b_{93} \\ Y_3 = \left(b_{33} + B_{33}\right) Q_{99} + \left(b_{99} + B_{99}\right) Q_{33} \\ \qquad -b_{93} Q_{39} - b_{39} Q_{93} \\ Y_4 = Q_{33} + Q_{99} + Q_{39} + Q_{93} \end{cases} \tag{10}$$

where the subscripts *r* and *i* denote the real and imaginary parts of the excitation forces f_3 and f_9, respectively.

Based on (9), an optimized PTO damping for maximizing the wave energy conversion for the wave of a given frequency and the corresponding maximized power conversion can be given, respectively, as follows:

$$B_{\text{pto}} = \sqrt{\frac{X_1^2 + \omega^2 Y_1^2}{X_2^2 + \omega^2 Y_2^2}} \tag{11}$$

$$\bar{P}_{\max} = \frac{1}{4} \frac{Z_1^2 + Z_2^2}{X_1 X_2 + \omega^2 Y_1 Y_2 + \sqrt{\left(X_1^2 + \omega^2 Y_1^2\right)\left(X_2^2 + \omega^2 Y_2^2\right)}}. \tag{12}$$

It can be seen that both the optimized PTO damping and the maximal converted wave energy are depending on frequency, hence this optimized condition may only be useful in the regular waves, where the wave frequencies are constant for a given wave.

2) PTO Optimization for Irregular Waves: Real sea waves, which are essentially irregular waves, differ from the idealized regular waves as discussed before, and generally can be considered as a combination of many regular wave components with different frequencies, amplitudes, and phases for a given point. The irregular waves are often characterized by wave spectrum shapes, significant wave heights, and characteristic periods (and wave spreading functions for the real wind-generated waves). Hence, the optimization of the PTO for irregular waves of a given sea state is not as simple as that given in Section III-B1.

As in any given sea state, the waves consist of different frequencies and amplitudes. Hence, the PTO damping must be optimized for the given sea state, rather than the individual waves. For a given PTO damping, the power response is given by (9), and from that the average power conversion for the sea state can be calculated as follows:

$$P_{\text{irr}} = 2 \int_0^\infty \bar{P} S(\omega) d\omega \tag{13}$$

where $S(\omega)$ is the wave spectrum (can be either theoretical or measured wave spectra).

The optimization of the PTO damping for a sea state is dependent on the PTO damping level, and the PTO damping corresponding to the max wave energy conversion is given by (13), which is taken as the optimized damping for the irregular waves for the theoretical and measured wave spectra.

To simplify practical applications, theoretical wave spectra have been developed and are widely used in WEC development. The most popular theoretical wave spectra are the JONSWAP and Bretschneider spectra: The former is generally considered as the waves are not fully developed in coastal areas in terms of either limited fetch or limited wind blow duration, whereas the latter is used for fully developed wind-generated waves in open seas without limits of fetch or wind blow duration. However, it should be noted that in west coast of Ireland, the waves may very likely have propagated a long distance from the Atlantic or generated by local winds or a combination of both.

A generalised JONSWAP spectrum can be given by following the formula in [23]

$$\mathrm{S}(\omega) = (1 - 0.287 \ln \gamma) \frac{5}{16} H_s^2 \frac{\omega_p^4}{\omega^5} \exp\left(-\frac{5}{4}\frac{\omega_p^4}{\omega^4}\right) \times \gamma^\alpha \tag{14}$$

where $\omega_p = 2\pi/T_p$, $\alpha = \exp[-(\omega - \omega_p)^2 / 2\omega_p^2 \sigma^2]$, $\sigma = \begin{cases} 0.07, & \text{if } \omega \le \omega_p \\ 0.09, & \text{if } \omega > \omega_p \end{cases}$, and γ is the peakness factor of the spectrum. For the Bretschneider spectrum $\gamma = 1$, while the standard JONSWAP given by $\gamma = 3.3$. In addition, the statistical periods can be calculated by following [23]:

$$T_e = \frac{4.2 + \gamma}{5 + \gamma} T_p;\ T_{01} = \frac{5 + \gamma}{6.8 + \gamma} T_p;\ T_{02} = \sqrt{\frac{5 + \gamma}{11 + \gamma}} T_p. \tag{15}$$

IV. Wave Energy Conversion of RM3

A. Wave Resource and Climate

The scatter plot showing the occurrence of the various wave conditions on the AMETS site in 2010 is shown in Fig. 3. As it can be seen the most dominant wave condition occurs at a significant wave height of 1.75 m and an energy period of 8.75 s, with a max occurrence of 3.71%. The analysis shows that 98.1% of all waves occurs in a range of 0.75 to 7.75 m significant wave heights (H_s) and 4.75 to 12.25 s energy period (T_e).

The site shows several occurrences where the significant wave heights, H_s, are more than 8 m (less than 0.4% occurrence). These conditions are generally regarded as severe storm conditions and this will need to be considered as an important factor in the design because the devices must survive from these severe conditions in their deployment period.

B. Power Capture From Different Spectra

This section presents the results for the power capture of the RM3 device in irregular waves of different types of wave spectra, including the standard JONSWAP, Bretschneider, and the real measured wave spectra. These different types of wave spectra are characterized with same significant wave height, H_s, and wave energy period, T_e, and thus the same wave energy levels, but their bandwidths of the wave density spectra can be different. For instance, the standard JONSWAP spectrum has a much more wave energy concentrated around the spectral peak period than that of Bretschneider. In reality, most of wave energy converters are narrowly banded, meaning that the wave energy converters are very efficient in converting wave energy from the waves with certain frequencies (in a narrow bandwidth), while they are very inefficient for waves out of this narrow frequency bandwidth. Hence, it is very likely that the wave energy converters can extract different wave energy from waves of different density spectra. In assessing wave energy conversion in irregular waves, (13) is the formula for calculating the converted wave energy by the device. However, unlike the cases for regular waves, the optimized B_{pto} for a given wave spectrum can be obtained indirectly by varying the PTO damping level (i.e., B_{pto}), and the

Power matrix	Energy period, Te (s)																				
Significant wave height, Hs (m)	4.25	4.75	5.25	5.75	6.25	6.75	7.25	7.75	8.25	8.75	9.25	9.75	10.25	10.75	11.25	11.75	12.25	12.75	13.25	13.75	14.25
14.25	800	800	800	800	800	800	800	800	800	800	800	800	800	800	800	800	800	800	800	800	800
13.75	800	800	800	800	800	800	800	800	800	800	800	800	800	800	800	800	800	800	800	800	800
13.25	800	800	800	800	800	800	800	800	800	800	800	800	800	800	800	800	800	800	800	800	800
12.75	800	800	800	800	800	800	800	800	800	800	800	800	800	800	800	800	800	800	800	800	800
12.25	800	800	800	800	800	800	800	800	800	800	800	800	800	800	800	800	800	800	800	800	800
11.75	800	800	800	800	800	800	800	800	800	800	800	800	800	800	800	800	800	800	800	800	800
11.25	800	800	800	800	800	800	800	800	800	800	800	800	800	800	800	800	800	800	800	800	800
10.75	800	800	800	800	800	800	800	800	800	800	800	800	800	800	800	800	800	800	800	800	800
10.25	800	800	800	800	800	800	800	800	800	800	800	800	800	800	800	800	800	800	800	800	800
9.75	800	800	800	800	800	800	800	800	800	800	800	800	800	800	800	800	800	800	800	800	800
9.25	800	800	800	800	800	800	800	800	800	800	800	800	800	800	800	800	800	800	800	800	800
8.75	800	800	800	800	800	800	800	800	800	800	800	800	800	800	800	800	800	800	800	800	800
8.25	800	800	800	800	800	800	800	800	800	800	800	800	800	800	800	800	800	800	800	800	719.8
7.75	800	800	800	800	800	800	800	800	800	800	800	800	800	800	800	800	800	800	794.3	709.3	635.2
7.25	800	800	800	800	800	800	800	800	800	800	800	800	800	800	800	800	800	782.2	695.2	620.7	555.9
6.75	699.1	764.1	800	800	800	800	800	800	800	800	800	800	800	800	800	800	768	678	602.6	538	481.9
6.25	599.4	655.1	757.7	800	800	800	800	800	800	800	800	800	800	800	800	753.1	658.5	581.3	516.6	461.3	413.1
5.75	507.3	554.5	641.3	722.4	800	800	800	800	800	800	800	800	800	800	741	637.4	557.3	492	437.3	390.4	349.7
5.25	422.9	462.2	534.6	602.2	669.2	741.7	800	800	800	800	800	800	800	732.1	617.7	531.4	464.6	410.2	364.5	325.5	291.5
4.75	346.2	378.4	437.7	493	547.8	607.1	678.9	775.1	800	800	800	800	725.9	599.3	505.7	435	380.3	335.8	298.4	266.4	238.6
4.25	277.2	302.9	350.4	394.7	438.5	486	543.5	620.5	726	800	800	710	581.1	479.8	404.8	348.2	304.5	268.8	238.9	213.3	191
3.75	215.8	235.8	272.8	307.3	341.4	378.4	423.1	483.1	565.3	644.8	641.8	552.8	452.4	373.5	315.2	271.1	237	209.3	186	166.1	148.7
3.25	162.1	177.1	204.9	230.8	256.5	284.2	317.8	362.8	424.6	484.3	482.1	415.2	339.8	280.6	236.7	203.6	178	157.2	139.7	124.7	111.7
2.75	116	126.8	146.7	165.2	183.6	203.5	227.5	259.8	304	346.8	345.2	297.3	243.3	200.9	169.5	145.8	127.5	112.5	100	89.3	80
2.25	77.7	84.9	98.2	110.6	122.9	136.2	152.3	173.9	203.5	232.1	231.1	199	162.9	134.5	113.5	97.6	85.3	75.3	67	59.8	53.5
1.75	47	51.4	59.4	66.9	74.4	82.4	92.1	105.2	123.1	140.4	139.8	120.4	98.5	81.3	68.6	59	51.6	45.6	40.5	36.2	32.4
1.25	24	26.2	30.3	34.1	37.9	42	47	53.7	62.8	71.6	71.3	61.4	50.3	41.5	35	30.1	26.3	23.3	20.7	18.5	16.5
0.75	8.6	9.4	10.9	12.3	13.7	15.1	16.9	19.3	22.6	25.8	25.7	22.1	18.1	14.9	12.6	10.8	9.5	8.4	7.4	6.6	5.9
0.25	1	1	1.2	1.4	1.5	1.7	1.9	2.1	2.5	2.9	2.9	2.5	2	1.7	1.4	1.2	1.1	0.9	0.8	0.7	0.7

Fig. 4. Power matrix for the RM3 for the JONSWAP spectrum.

maximal P_{irr} corresponds to the optimized B_{pto} (more details can be found in [17]).

1) JONSWAP Spectrum: The JONSWAP spectrum is defined by its higher spectral peak and narrow bandwidth. Due to this narrow bandwidth, the majority of the power available for the spectrum is within the narrow range of frequencies. This may be favorable for many wave energy converters, including the RM3 floating PA, because the devices themselves may have a narrow bandwidth in efficiently converting wave energy. In the case of RM3, the power matrix can be seen in Fig. 4 with a rated power at 800 kW (note that this is for research purpose, hence no PTO energy conversion efficiency is applied). By combining the wave climate given in Fig. 3, an annual energy production (AEP) of 1971.8 MWh can be obtained.

2) Bretschneider Spectrum: The Bretschneider spectrum has a wider bandwidth and a lower spectral peak than those of the standard JONSWAP spectrum. The wider bandwidth means that the bulk of the wave energy is distributed in a wider range of frequencies that can make the energy capture more difficult. The calculation of the power matrix for the Bretschnerider spectrum was carried out in a similar manner to that of the JONSWAP spectrum, assuming a rated power for the RM3 of 800 kW. The results of this show an AEP of 1670.4 MWh, lower than that of the JONSWAP spectrum. The power matrix calculated for the Bretschneider optimization is shown in Fig. 5.

3) Real Sea Spectrum: Unlike the above-mentioned cases for the theoretical wave spectra, the real sea spectrum analysis used the average of the measured spectra in each bin to determine the power available from each set of wave conditions. By applying the measured average spectrum in each bin, the wave energy conversion by the RM3 device can be calculated and the corresponding power matrix can be obtained, as shown in Fig. 6. Again, the same rated power for the RM3 was assumed 800 kW.

The resultant AEP from the analysis showed that there is an AEP of 1692.7 MWh for the real sea spectrum.

C. Summary of Wave Energy Captures

The energy capture factor is an important factor in the design of any WEC and more specifically, it is the percentage of the actual energy conversion over the device's energy conversion in full capacity (i.e., the rated power) in all sea states. The method of calculating the capture factor is given as follows:

$$\varepsilon = \frac{\text{AEP}}{\text{Rated\_power} * 8760} \tag{16}$$

where AEP should has the same units as the rated power.

From Table I, it can be seen that the sea states can be more accurately described using a Bretschneider spectrum over a JONSWAP spectrum. Using the Bretschneider spectrum, a slight under-estimation of AEP (1.3%) is observed, and its capture factors is also very similar to that of the real sea measurements (0.242 versus 0.238). When the JONSWAP spectrum is used, the AEP is over-estimated by 16.5%, and a larger energy capture factor is obtained (0.281 versus 0.242).

V. Results and Analysis

A. Measured Wave and Theoretical Wave Spectra

As shown in Section IV, for the wave data on the west coast of Ireland (in the year 2010), the Bretschneider spectrum gives a much more accurate result in assessing the AEP for the RM3 WEC than the JONSWAP spectrum. In this section an investigation as to why this is the case is presented.

1) Annually Average Spectrum of Waves: The first case looks at the overall characteristics of the wave spectrum from the wave measurements. In this case, all the measured wave spectra are

Power matrix	Energy period, Te (s)																				
Significant wave height, Hs (m)	4.25	4.75	5.25	5.75	6.25	6.75	7.25	7.75	8.25	8.75	9.25	9.75	10.25	10.75	11.25	11.75	12.25	12.75	13.25	13.75	14.25
14.25	800	800	800	800	800	800	800	800	800	800	800	800	800	800	800	800	800	800	800	800	800
13.75	800	800	800	800	800	800	800	800	800	800	800	800	800	800	800	800	800	800	800	800	800
13.25	800	800	800	800	800	800	800	800	800	800	800	800	800	800	800	800	800	800	800	800	800
12.75	800	800	800	800	800	800	800	800	800	800	800	800	800	800	800	800	800	800	800	800	800
12.25	800	800	800	800	800	800	800	800	800	800	800	800	800	800	800	800	800	800	800	800	800
11.75	800	800	800	800	800	800	800	800	800	800	800	800	800	800	800	800	800	800	800	800	800
11.25	800	800	800	800	800	800	800	800	800	800	800	800	800	800	800	800	800	800	800	800	800
10.75	800	800	800	800	800	800	800	800	800	800	800	800	800	800	800	800	800	800	800	800	800
10.25	800	800	800	800	800	800	800	800	800	800	800	800	800	800	800	800	800	800	800	800	800
9.75	800	800	800	800	800	800	800	800	800	800	800	800	800	800	800	800	800	800	800	800	800
9.25	800	800	800	800	800	800	800	800	800	800	800	800	800	800	800	800	800	800	800	800	800
8.75	800	800	800	800	800	800	800	800	800	800	800	800	800	800	800	800	800	800	800	800	800
8.25	800	800	800	800	800	800	800	800	800	800	800	800	800	800	800	800	800	800	800	800	800
7.75	783	800	800	800	800	800	800	800	800	800	800	800	800	800	800	800	800	800	800	800	800
7.25	685.2	754.3	800	800	800	800	800	800	800	800	800	800	800	800	800	800	800	800	800	800	800
6.75	594	653.8	763.7	800	800	800	800	800	800	800	800	800	800	800	800	800	800	800	800	780.4	706
6.25	509.2	560.5	654.7	740.6	800	800	800	800	800	800	800	800	800	800	800	800	800	800	738.6	669.1	605.3
5.75	431	474.4	554.1	626.8	696.3	767.1	800	800	800	800	800	800	800	800	800	800	755.4	688.3	625.1	566.3	512.3
5.25	359.3	395.5	462	522.6	580.5	639.5	704.7	776.5	800	800	800	800	800	800	744.5	687.6	629.7	573.8	521.1	472.1	427.1
4.75	294.1	323.8	378.2	427.8	475.2	523.5	576.9	635.6	688.8	722.8	732.5	721.2	693.4	654.9	609.5	562.9	515.5	469.7	426.6	386.5	349.6
4.25	235.5	259.2	302.7	342.5	380.4	419.1	461.8	508.8	551.4	578.7	586.4	577.3	555.1	524.3	487.9	450.6	412.7	376	341.5	309.4	279.9
3.75	183.3	201.8	235.7	266.6	296.2	326.3	359.6	396.2	429.3	450.5	456.6	449.5	432.2	408.2	379.9	350.8	321.3	292.7	265.9	240.9	217.9
3.25	137.7	151.6	177	200.3	222.4	245.1	270.1	297.6	322.4	338.4	342.9	337.6	324.6	306.6	285.3	263.5	241.3	219.9	199.7	180.9	163.7
2.75	98.6	108.5	126.8	143.4	159.3	175.5	193.4	213	230.9	242.3	245.5	241.7	232.4	219.5	204.3	188.7	172.8	157.4	143	129.5	117.2
2.25	66	72.6	84.9	96	106.6	117.5	129.4	142.6	154.5	162.2	164.4	161.8	155.6	146.9	136.7	126.3	115.7	105.4	95.7	86.7	78.4
1.75	39.9	43.9	51.3	58.1	64.5	71.1	78.3	86.3	93.5	98.1	99.4	97.9	94.1	88.9	82.7	76.4	70	63.8	57.9	52.5	47.5
1.25	20.4	22.4	26.2	29.6	32.9	36.3	40	44	47.7	50.1	50.7	49.9	48	45.4	42.2	39	35.7	32.5	29.5	26.8	24.2
0.75	7.3	8.1	9.4	10.7	11.8	13.1	14.4	15.8	17.2	18	18.3	18	17.3	16.3	15.2	14	12.9	11.7	10.6	9.6	8.7
0.25	0.8	0.9	1	1.2	1.3	1.5	1.6	1.8	1.9	2	2	2	1.9	1.8	1.7	1.6	1.4	1.3	1.2	1.1	1

Fig. 5. Power Matrix for the device for the Bretschneider spectrum.

Power matrix	Energy period, Te (s)																				
Significant wave height, Hs (m)	4.25	4.75	5.25	5.75	6.25	6.75	7.25	7.75	8.25	8.75	9.25	9.75	10.25	10.75	11.25	11.75	12.25	12.75	13.25	13.75	14.25
14.25	800	800	800	800	800	800	800	800	800	800	800	800	800	800	800	800	800	800	800	800	800
13.75	800	800	800	800	800	800	800	800	800	800	800	800	800	800	800	800	800	800	800	800	800
13.25	800	800	800	800	800	800	800	800	800	800	800	800	800	800	800	800	800	800	800	800	800
12.75	800	800	800	800	800	800	800	800	800	800	800	800	800	800	800	800	800	800	800	800	800
12.25	800	800	800	800	800	800	800	800	800	800	800	800	800	800	800	800	800	800	800	800	800
11.75	800	800	800	800	800	800	800	800	800	800	800	800	800	800	800	800	800	800	800	800	800
11.25	800	800	800	800	800	800	800	800	800	800	800	800	800	800	800	800	800	800	800	800	800
10.75	800	800	800	800	800	800	800	800	800	800	800	800	800	800	800	800	800	800	800	800	800
10.25	800	800	800	800	800	800	800	800	800	800	800	800	800	800	800	800	800	800	800	800	800
9.75	800	800	800	800	800	800	800	800	800	800	800	800	800	800	800	800	800	800	800	800	800
9.25	800	800	800	800	800	800	800	800	800	800	800	800	800	800	800	800	800	800	800	800	800
8.75	800	800	800	800	800	800	800	800	800	800	800	800	800	800	800	800	800	800	800	800	800
8.25	800	800	800	800	800	800	800	800	800	800	800	800	800	800	800	800	800	800	800	800	800
7.75	783	800	800	800	800	800	800	800	800	800	800	800	800	800	800	800	800	800	800	800	800
7.25	685.2	754.3	800	800	800	800	800	800	800	800	800	800	800	800	800	800	800	800	800	800	761.9
6.75	594	653.8	763.7	800	800	800	800	800	800	800	800	800	800	800	800	800	800	800	639.9	800	696.9
6.25	509.2	560.5	654.7	740.6	800	800	800	800	800	800	800	800	800	800	800	800	769.3	624.7	576.7	569.9	589.4
5.75	431	474.4	554.1	626.8	696.3	767.1	800	800	800	800	800	800	800	800	800	716.7	624.2	508.7	471.1	566.3	512.3
5.25	359.3	395.5	462	522.6	580.5	639.5	704.7	776.5	800	800	800	800	800	741.2	701.7	644.6	489.7	390.3	521.1	472.1	427.1
4.75	294.1	323.8	378.2	427.8	475.2	523.5	576.9	635.6	769.8	793.5	800	782.6	701.4	618.6	556.7	496	450.8	421.5	426.6	386.5	349.6
4.25	235.5	259.2	302.7	342.5	380.4	419.1	458.3	498.6	603.6	650.6	637.8	591.2	560.3	506.7	449.7	416.3	391.4	376	341.5	309.4	279.9
3.75	183.3	201.8	235.7	266.6	296.2	326.3	316.1	405.5	444.9	490.1	490.4	482.6	431.3	395.7	367.9	343.8	326.9	292.7	213.2	229.5	234.8
3.25	137.7	151.6	177	200.3	222.4	223.9	243.7	284.9	333.6	351.8	360.7	356.1	335.1	321.9	263.7	231.7	219.6	193.7	172.6	180.9	163.7
2.75	98.6	108.5	126.8	143.4	139.5	156.2	172	202.9	228	249.9	265	252.7	242.9	213.3	197.1	171.8	151.3	134.7	128.7	105.7	96.9
2.25	66	72.6	62.3	84.1	88.7	100.1	117.9	135.2	152.2	164.8	177	175.7	166.9	152.1	133.3	102.8	111.4	92.4	87	79.8	66.4
1.75	39.9	43.9	37	44.9	55.5	60.3	71.2	81.1	92.3	100.5	106.2	112.9	99.2	83.3	72.4	70.6	66.8	55.5	45.2	52.5	49.8
1.25	20.4	12.2	22	25.5	27.3	32.3	36.9	44.5	49.9	54.5	60.3	59.6	55	45.7	45.9	30.3	21.2	22.7	29.5	26.8	24.2
0.75	7.3	5.5	8.4	11.5	13.1	13.9	15.5	17.3	18.7	20.7	22.6	24.6	20.7	22.5	17.2	14	9.7	11.7	10.6	9.6	8.7
0.25	0.8	0.9	1	1.2	1.3	1.5	1.6	1.8	0.3	2	2	2	1.9	1.8	1.7	1.6	1.4	1.3	1.2	1.1	1

Fig. 6. Power matrix for the real sea states for the RM3.

TABLE I
ANNUAL ENERGY CAPTURE AND CAPTURE FACTORS

Wave spectrum	AEP (MWh)	Gain (%)	Capture factor, ε
Measured wave	1692.7	-	0.242
JONSWAP	1971.8	16.5	0.281
Bretschneider	1670.4	-1.3	0.238

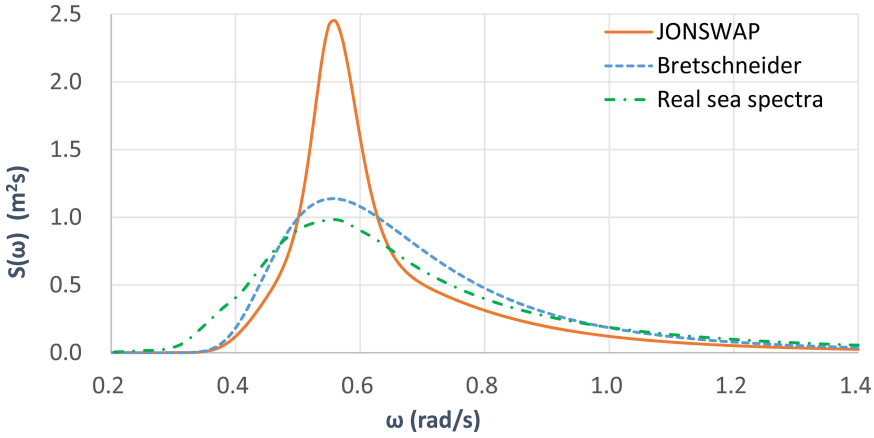

Fig. 7. Spectra comparison (theoretical spectrum and measured spectrum).

TABLE II
BANDWIDTH PARAMETERS FOR THE MEASURED AVERAGE WAVE SPECTRA

Case	Low cut-off frequency (rad/s)	High cut-off frequency (rad/s)	Bandwidth	Note
1	0.157	2.262	0.4406	Cut-off by $4\omega_{\mathrm{p}}$
2	0.157	2.827	0.4876	Cut-off by $5\omega_{\mathrm{p}}$

average and it can be seen that the overall average spectrum is very smooth (see Fig. 7, "green dashed-dot line"). Taking the significant wave height and the spectral peak period from the average spectrum of the measured waves, the corresponding Bretschneider and JONSWAP spectra are plotted for comparison (see Fig. 7). From the spectral shapes, it can be clearly seen that the Bretschneider spectrum is a much closer fit to the real sea spectrum than the JONSAWP spectrum.

It can also be seen that the measured average spectrum has larger values in the lower frequencies and smaller values in higher frequencies than those of theoretical spectra. The reason for this is that the measured spectra may contain both the Atlantic swells (waves with long periods) and local wind generated waves (waves with relative short periods). As such, the measured individual wave spectra may have double peaks (can be seen in some examples next), while the theoretical spectra have only one peak.

The spectral bandwidth of the waves was also examined. Following [24], the most popular spectral bandwidth is defined as follows:

$$\nu = \sqrt{\frac{\mathrm{m_0 m_2}}{\mathrm{m_1^2}} - 1}. \tag{17}$$

For the Bretschneider spectrum $\nu = 0.425$, and for the standard JONSWAP spectrum with $\gamma = 3.3$, $\nu = 0.39$.

In calculating the spectral bandwidth for measured waves, it is important to decide the cutoff of the low and high frequencies. Following the suggestion in [24], the high cutoff frequency has been suggested to be in the region of $4\omega_{\mathrm{p}}$ and $5\omega_{\mathrm{p}}$. Table II presents the measured wave spectral bandwidths for the different cutoff frequencies. Again, the bandwidth factor is closer to that of Bretschneider than the JONSWAP spectrum.

2) Most Happened Sea States: The second case examined focuses on the bin with the most happened sea states. In this case, the bin: $H_s = 1.75$ m (range: 1.5–2.0 m), $T_e = 8.75$ s (range: 8.5–9.0 s), there are a total 489 waves (see Fig. 8; some of the measured spectra are plotted against the average spectrum). It can be seen that individual spectra vary significantly with different peaks and bandwidths, and some showing the aforementioned double spectral peaks.

In Fig. 9, a comparison is made for the average most happened wave spectrum and the corresponding theoretical spectrum (JONSWAP and Bretschneider). Again, it can be seen that the measured spectrum is close to the Bretschneider spectrum. When the peakness factor $\gamma = 1.14$, the modified JONSWAP spectrum is similar to the average spectrum of the most happened sea states (see Fig. 10). Table III gives the bandwidth factor comparison between the most happened spectra and the theoretical spectra.

3) Most Energetic Sea States: In this case, we examine the most energetic sea states, and this occurs in the bin $\mathrm{H_s} = 3.25$ m (range: 3.0–3.5 m) and $T_e = 9.25$ s (range: 9.0–9.5 s). The most energetic sea states mean the total annual wave energy in the bin is the largest, which is calculated by wave occurrence multiplied by the wave energy density in the bin.

Figure 11 shows the some of the 272 individual spectra in the bin and the average spectrum. Similar to the bin of the most happened sea states, the individual wave spectra vary largely in peak and bandwidth (some showing double spectral peaks), although the average wave spectrum is very smooth.

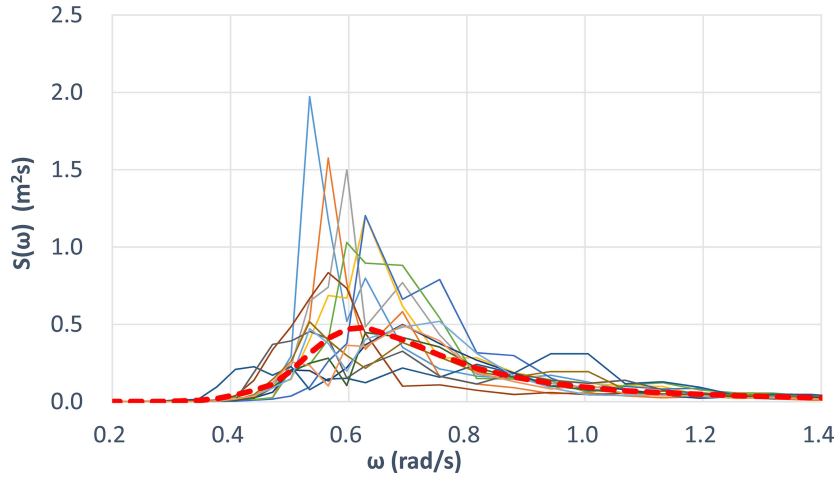

Fig. 8. Part of the measured spectra from the bin containing the most occurred waves totaling 489 spectra, the average spectrum shown as the red dashed line.

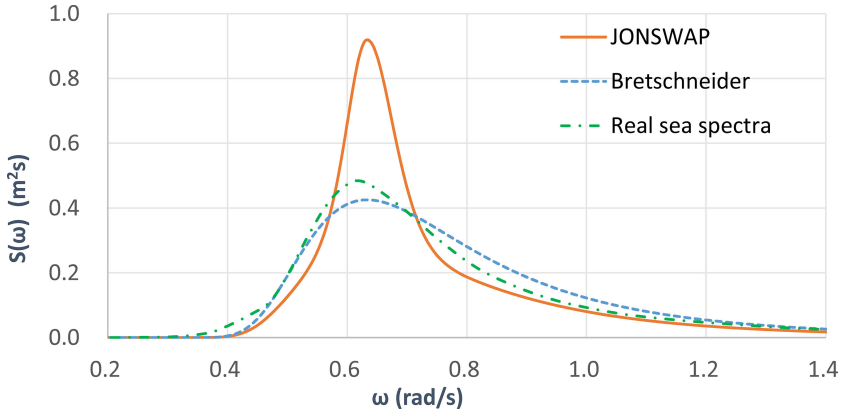

Fig. 9. Spectra comparison between JONSWAP, Bretschneider, and the most occurred sea spectra (average).

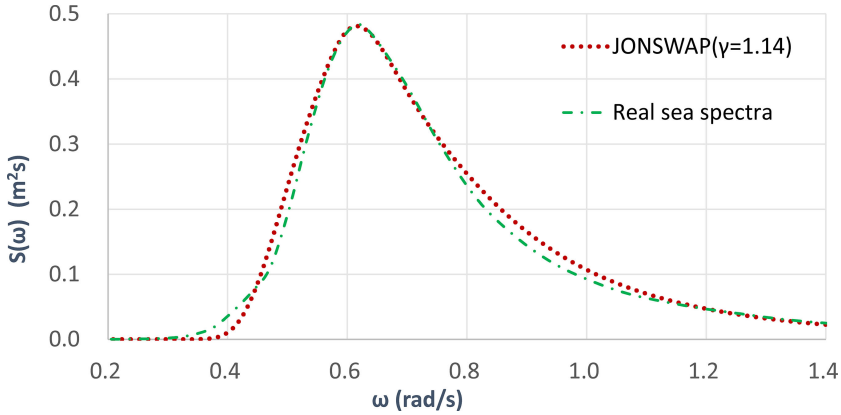

Fig. 10. Average spectrum for the most happened waves and the modified JONSWAP spectrum ($\gamma = 1.14$).

The comparison of the measured wave spectrum and the Bretschneider and JONSWAP spectra can be seen in Fig. 12. The measured average spectrum has a slightly higher peak than that of the Bretschneider spectrum. When the peakness factor $\gamma = 1.25$, the JONSWAP spectra is close to the highest AEP average spectra (Fig. 13). Table IV gives the bandwidth factor comparison between the most happened spectra and the theoretical spectra.

B. Power Performance Curves

Through using the different theoretical spectra, the power performance of the RM3 device will have different characteristics (here, power performance curve is defined as the maximized power conversion for a given sea state of $H_s = 2$ m, (i.e., the unit significant wave amplitude) and the wave energy period T_e under the given spectral types). Fig. 14 shows the comparison of

TABLE III
BANDWIDTH PARAMETERS FOR THE MOST HAPPENED MEASURED AVERAGE WAVE SPECTRA

Case	Low cut-off frequency (rad/s)	High cut-off frequency (rad/s)	Bandwidth	Note
1	0.157	2.262	0.3914	Cut-off by $4\omega_p$
2	0.157	2.827	0.4523	Cut-off by $5\omega_p$
3	-	-	0.4218	Theoretical spectrum, $\gamma = 1.14$

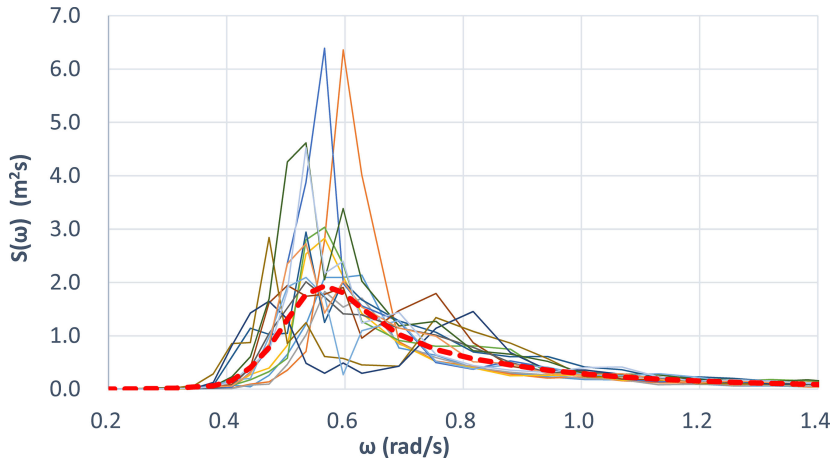

Fig. 11. Part of the measured spectra from the most energetic bin. Average spectrum shown as the red dashed line.

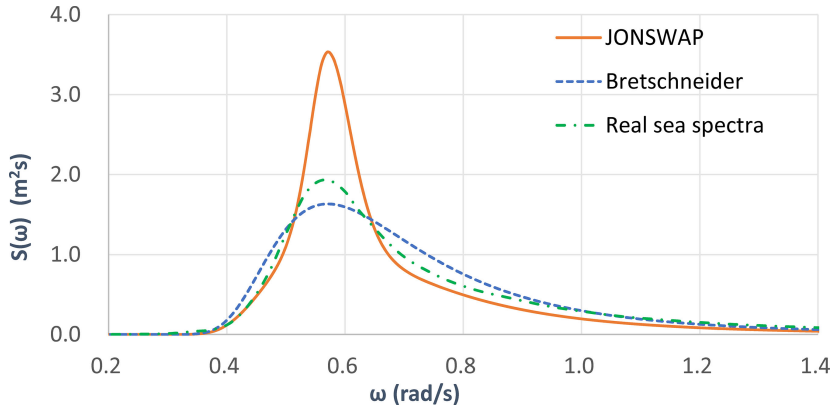

Fig. 12. Spectra comparison between JONSWAP, Bretschneider, and the highest AEP average Real Sea Spectra.

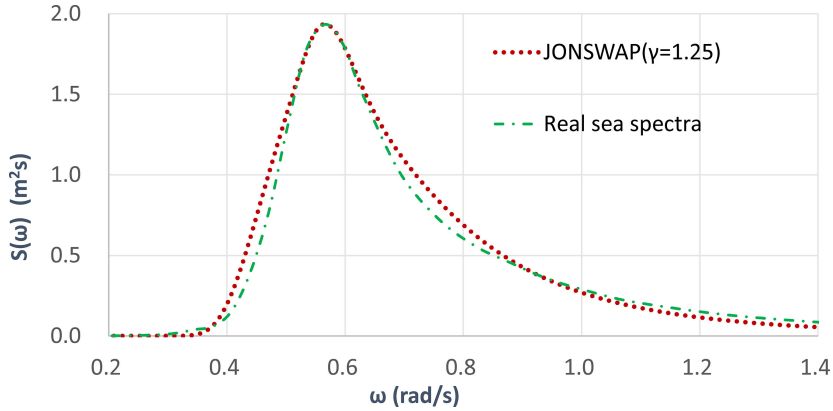

Fig. 13. Average spectrum for the most energetic binned waves and the modified JONSWAP spectrum ($\gamma = 1.25$).

TABLE IV
BANDWIDTH PARAMETERS FOR THE HIGHEST AEP AVERAGE WAVE SPECTRA

Case	Low cut-off frequency (rad/s)	High cut-off frequency (rad/s)	Bandwidth	Note
1	0.157	2.262	0.4152	Cut-off by $4\omega_p$
2	0.157	2.827	0.4596	Cut-off by $5\omega_p$
3	-	-	0.4200	Theoretical spectrum, $\gamma = 1.25$

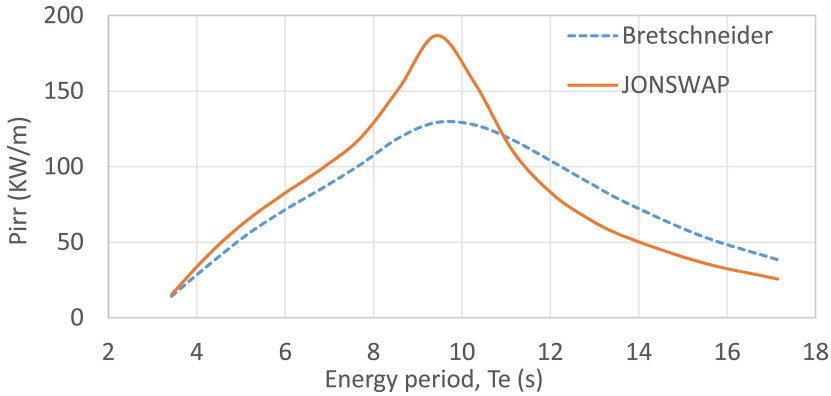

Fig. 14. Two theoretical spectra used in the analysis and their respective power curves.

MWh	Energy period, Te (s)																				
Significant wave height, Hs (m)	4.25	4.75	5.25	5.75	6.25	6.75	7.25	7.75	8.25	8.75	9.25	9.75	10.25	10.75	11.25	11.75	12.25	12.75	13.25	13.75	14.25
14.25	0	0	0	0	0	0	0	0	0	0	0	0	0	0	0	0	0	0	0	0	0
13.75	0	0	0	0	0	0	0	0	0	0	0	0	0	0	0	0	0	0	0	0	0
13.25	0	0	0	0	0	0	0	0	0	0	0	0	0	0	0	0	0	0	0	0	0
12.75	0	0	0	0	0	0	0	0	0	0	0	0	0	0	0	0	0	0	0	0	0
12.25	0	0	0	0	0	0	0	0	0	0	0	0	0	0	0	0	0	0	0	0	0
11.75	0	0	0	0	0	0	0	0	0	0	0	0	0	0	0	0	0	0	0	0	0
11.25	0	0	0	0	0	0	0	0	0	0	0	0	0	0	0	0	0	0	0	0	0
10.75	0	0	0	0	0	0	0	0	0	0	0	0	0	0	0	0	0	0	0	0	0
10.25	0	0	0	0	0	0	0	0	0	0	0	0	0	0	0	0	0	0	0	0	0
9.75	0	0	0	0	0	0	0	0	0	0	0	0	0	0	0	0	0	0	0	0	0
9.25	0	0	0	0	0	0	0	0	0	0	0	0	0	0	0	0	0	0	0	0	0
8.75	0	0	0	0	0	0	0	0	0	0	0	0	0	0	0	0	0	0	0	0	0
8.25	0	0	0	0	0	0	0	0	0	0	0	0	0	0	0	0	0	0	0	0	0.07
7.75	0	0	0	0	0	0	0	0	0	0	0	0	0	0	0	0	0	0	0.005	0.079	0
7.25	0	0	0	0	0	0	0	0	0	0	0	0	0	0	0	0	0	0.078	0.184	0	0.214
6.75	0	0	0	0	0	0	0	0	0	0	0	0	0	0	0	0	0.252	0.641	0.346	0.212	0.196
6.25	0	0	0	0	0	0	0	0	0	0	0	0	0	0	0	0.452	1.116	0.192	0.389	0.364	0.168
5.75	0	0	0	0	0	0	0	0	0	0	0	0	0	0	0.724	1.709	0.521	0.344	0.329	0	0
5.25	0	0	0	0	0	0	0	0	0	0	0	0	0	1.249	1.555	1.505	0.434	0.287	0	0	0
4.75	0	0	0	0	0	0	0	0	−0.58	−0.74	−1.66	−2.35	−1	1.51	2	1.569	0.592	0.235	0	0	0
4.25	0	0	0	0	0	0	−0.07	−0.78	−1.84	−10.1	−11.2	−8.37	−1.07	1.053	1.456	1.076	0.758	0	0	0	0
3.75	0	0	0	0	0	0	−0.22	−1.22	−5.96	−14.1	−15.4	−7.78	−0.97	1.581	2.097	0.698	0.222	0	0.35	0.066	0.061
3.25	0	0	0	0	0	−0.24	−0.46	−2.91	−7.97	−19	−25.1	−10.7	−1.4	1.549	2.171	1.784	0.555	0.439	0.263	0	0
2.75	0	0	0	0	−0.19	−0.52	−2.21	−4.71	−13.7	−23.9	−22.5	−7.7	−1.1	1.466	1.707	1.466	1.032	0.354	0.377	0.07	0.033
2.25	0	0	−0.01	−0.03	−0.24	−0.93	−3.43	−5.57	−9.23	−14.8	−10.9	−4.99	−0.75	0.739	0.732	0.528	0.373	0.396	0.327	0.212	0.065
1.75	0	0	−0.08	−0.52	−0.94	−1.72	−2.33	−4.65	−8.89	−13.7	−9.48	−3.53	−0.44	0.326	0.247	0.259	0.161	0.048	0.03	0	0.013
1.25	0	−0.01	−0.17	−0.53	−0.4	−0.75	−1.34	−2.02	−4.1	−4.22	−4.11	−1.75	−0.21	0.188	0.126	0.023	0.041	0.04	0	0	0
0.75	0	−0.01	−0.02	−0.08	−0.05	−0.12	−0.21	−0.24	−0.23	−0.23	−0.26	−0.05	−0	0.004	0.005	0	0.003	0	0	0	0
0.25	0	0	0	0	0	0	0	0	−0	0	0	0	0	0	0	0	0	0	0	0	0

Fig. 15. Bretschneider spectrum gain/loss matrix compared to the JONSWAP spectrum for power capture.

the power performance curves for the Bretschneider and JONSWAP spectra. It can be seen that using the JONWAP spectrum, the RM3 power performance curve is larger than that of the Bretshneider spectrum for the wave energy period less than 11 s, and a large difference occurs at $T_e = 9.5$ s, when the JONSWAP spectrum gives 40% more converted energy compared to that from the Bretschnerider spectrum.

When the wave energy period is longer than 11 s, the RM3 extracts more wave energy from the Bretschneider spectrum than from the JONSWAP spectrum. It should be noted that for the wave scatter diagram in Fig. 3, about 81% of waves occurred at wave energy periods less than 11 s, and these waves are more significant for wave energy conversion.

C. Power Estimations for Different Spectra

In this section, the power differences are given for the bins where different spectra are used.

1) Theoretical Spectra: We use the JONSWAP and Bretschneider spectra to assess the AEP for the RM3 device

MWh	Energy period, Te (s)																			
Significant wave height, Hs (m)	4.25	4.75	5.25	5.75	6.25	6.75	7.25	7.75	8.25	8.75	9.25	9.75	10.25	10.75	11.25	11.75	12.25	12.75	13.25	13.75	14.25
14.25	0	0	0	0	0	0	0	0	0	0	0	0	0	0	0	0	0	0	0	0	0
13.75	0	0	0	0	0	0	0	0	0	0	0	0	0	0	0	0	0	0	0	0	0
13.25	0	0	0	0	0	0	0	0	0	0	0	0	0	0	0	0	0	0	0	0	0
12.75	0	0	0	0	0	0	0	0	0	0	0	0	0	0	0	0	0	0	0	0	0
12.25	0	0	0	0	0	0	0	0	0	0	0	0	0	0	0	0	0	0	0	0	0
11.75	0	0	0	0	0	0	0	0	0	0	0	0	0	0	0	0	0	0	0	0	0
11.25	0	0	0	0	0	0	0	0	0	0	0	0	0	0	0	0	0	0	0	0	0
10.75	0	0	0	0	0	0	0	0	0	0	0	0	0	0	0	0	0	0	0	0	0
10.25	0	0	0	0	0	0	0	0	0	0	0	0	0	0	0	0	0	0	0	0	0
9.75	0	0	0	0	0	0	0	0	0	0	0	0	0	0	0	0	0	0	0	0	0
9.25	0	0	0	0	0	0	0	0	0	0	0	0	0	0	0	0	0	0	0	0	0
8.75	0	0	0	0	0	0	0	0	0	0	0	0	0	0	0	0	0	0	0	0	0
8.25	0	0	0	0	0	0	0	0	0	0	0	0	0	0	0	0	0	0	0	0	0
7.75	0	0	0	0	0	0	0	0	0	0	0	0	0	0	0	0	0	0	0	0	0
7.25	0	0	0	0	0	0	0	0	0	0	0	0	0	0	0	0	0	0	0	0	−0.03
6.75	0	0	0	0	0	0	0	0	0	0	0	0	0	0	0	0	0	0	−0.28	0.017	−0.01
6.25	0	0	0	0	0	0	0	0	0	0	0	0	0	0	0	0	−0.24	−0.15	−0.28	−0.17	−0.01
5.75	0	0	0	0	0	0	0	0	0	0	0	0	0	0	0	−0.88	−0.34	−0.31	−0.27	0	0
5.25	0	0	0	0	0	0	0	0	0	0	0	0	0	−1.08	−0.52	−0.41	−0.37	−0.32	0	0	0
4.75	0	0	0	0	0	0	0	0	0.426	0.681	1.656	1.829	0.245	−0.99	−1.02	−0.82	−0.28	−0.08	0	0	0
4.25	0	0	0	0	0	0	−0	−0.07	0.549	3.275	2.702	0.877	0.214	−0.42	−0.67	−0.36	−0.15	0	0	0	0
3.75	0	0	0	0	0	0	−0.15	0.13	0.683	2.879	2.813	2.494	−0.04	−0.57	−0.39	−0.06	0.015	0	−0.23	−0.01	0.015
3.25	0	0	0	0	0	−0.13	−0.25	−0.57	0.873	1.749	3.212	2.544	0.966	0.911	−0.97	−0.95	−0.19	−0.18	−0.12	0	0
2.75	0	0	0	0	−0.16	−0.36	−1.39	−1.02	−0.54	1.738	4.407	1.522	1.058	−0.49	−0.35	−0.58	−0.49	−0.18	−0.13	−0.04	−0.02
2.25	0	0	−0.02	−0.02	−0.27	−0.87	−1.72	−1.32	−0.43	0.551	2.064	1.863	1.168	0.31	−0.11	−0.43	−0.05	−0.17	−0.1	−0.05	−0.03
1.75	0	0	−0.14	−0.77	−0.85	−1.65	−1.2	−1.28	−0.36	0.78	1.596	2.352	0.514	−0.24	−0.18	−0.09	−0.03	−0.02	−0.02	0	0.002
1.25	0	−0.02	−0.17	−0.48	−0.45	−0.53	−0.59	0.104	0.597	0.863	1.917	1.479	0.625	0.014	0.065	−0.02	−0.06	−0.04	0	0	0
0.75	0	−0.02	−0.01	0.039	0.034	0.05	0.092	0.104	0.064	0.078	0.151	0.081	0.018	0.016	0.004	0	−0	0	0	0	0
0.25	0	0	0	0	0	0	0	0	−0	0	0	0	0	0	0	0	0	0	0	0	0

Fig. 16. Wave conditions where the real sea spectrum has a gain/loss over the Bretschneider spectrum for power capture.

MWh	Energy period, Te (s)																			
Significant wave height, Hs (m)	4.25	4.75	5.25	5.75	6.25	6.75	7.25	7.75	8.25	8.75	9.25	9.75	10.25	10.75	11.25	11.75	12.25	12.75	13.25	13.75	14.25
14.25	0	0	0	0	0	0	0	0	0	0	0	0	0	0	0	0	0	0	0	0	0
13.75	0	0	0	0	0	0	0	0	0	0	0	0	0	0	0	0	0	0	0	0	0
13.25	0	0	0	0	0	0	0	0	0	0	0	0	0	0	0	0	0	0	0	0	0
12.75	0	0	0	0	0	0	0	0	0	0	0	0	0	0	0	0	0	0	0	0	0
12.25	0	0	0	0	0	0	0	0	0	0	0	0	0	0	0	0	0	0	0	0	0
11.75	0	0	0	0	0	0	0	0	0	0	0	0	0	0	0	0	0	0	0	0	0
11.25	0	0	0	0	0	0	0	0	0	0	0	0	0	0	0	0	0	0	0	0	0
10.75	0	0	0	0	0	0	0	0	0	0	0	0	0	0	0	0	0	0	0	0	0
10.25	0	0	0	0	0	0	0	0	0	0	0	0	0	0	0	0	0	0	0	0	0
9.75	0	0	0	0	0	0	0	0	0	0	0	0	0	0	0	0	0	0	0	0	0
9.25	0	0	0	0	0	0	0	0	0	0	0	0	0	0	0	0	0	0	0	0	0
8.75	0	0	0	0	0	0	0	0	0	0	0	0	0	0	0	0	0	0	0	0	0
8.25	0	0	0	0	0	0	0	0	0	0	0	0	0	0	0	0	0	0	0	0	−0.07
7.75	0	0	0	0	0	0	0	0	0	0	0	0	0	0	0	0	0	0	−0	−0.08	0
7.25	0	0	0	0	0	0	0	0	0	0	0	0	0	0	0	0	0	−0.08	−0.18	0	−0.18
6.75	0	0	0	0	0	0	0	0	0	0	0	0	0	0	0	0	−0.25	−0.64	−0.07	−0.23	−0.19
6.25	0	0	0	0	0	0	0	0	0	0	0	0	0	0	0	−0.45	−0.87	−0.04	−0.11	−0.19	−0.15
5.75	0	0	0	0	0	0	0	0	0	0	0	0	0	0	−0.72	−0.83	−0.18	−0.03	−0.06	0	0
5.25	0	0	0	0	0	0	0	0	0	0	0	0	0	−0.17	−1.03	−1.09	−0.07	0.035	0	0	0
4.75	0	0	0	0	0	0	0	0	0.159	0.063	0	0.518	0.751	−0.52	−0.98	−0.75	−0.31	−0.15	0	0	0
4.25	0	0	0	0	0	0	0.075	0.854	1.287	6.805	8.525	7.493	0.856	−0.64	−0.79	−0.72	−0.61	0	0	0	0
3.75	0	0	0	0	0	0	0.375	1.088	5.274	11.25	12.6	5.289	1.017	−1.01	−1.71	−0.64	−0.24	0	−0.12	−0.06	−0.08
3.25	0	0	0	0	0	0.37	0.714	3.48	7.095	17.29	21.91	8.128	0.432	−2.46	−1.21	−0.84	−0.36	−0.26	−0.14	0	0
2.75	0	0	0	0	0.348	0.87	3.598	5.732	14.25	22.15	18.13	6.173	0.04	−0.98	−1.35	−0.89	−0.54	−0.18	−0.25	−0.03	−0.01
2.25	0	0	0.031	0.046	0.509	1.803	5.153	6.882	9.662	14.27	8.862	3.123	−0.41	−1.05	−0.62	−0.1	−0.32	−0.22	−0.23	−0.16	−0.03
1.75	0	0	0.216	1.291	1.788	3.369	3.534	5.932	9.254	12.97	7.888	1.176	−0.07	−0.09	−0.07	−0.17	−0.13	−0.03	−0.01	0	−0.02
1.25	0	0.025	0.334	1.01	0.854	1.275	1.929	1.918	3.503	3.355	2.197	0.274	−0.42	−0.2	−0.19	−0	0.022	0.003	0	0	0
0.75	0	0.031	0.031	0.039	0.016	0.075	0.117	0.138	0.167	0.147	0.109	−0.03	−0.01	−0.02	−0.01	0	−0	0	0	0	0
0.25	0	0	0	0	0	0	0	0	0.002	0	0	0	0	0	0	0	0	0	0	0	0

Fig. 17. Wave conditions where the real sea spectrum has a gain/loss over the JONSWAP spectrum for power capture.

based on the power performance curve given in Fig. 14. Less wave energy conversions from Bretschneider spectrum can be seen when the energy period is less than 10.25 s (see Fig. 15), with a maximum difference at 25.1 MWh for the bin of $H_s = 3.25$ m and $T_e = 9.25$ s (coincidently, it is the most energetic bin also), while more power than that from JONSWAP spectrum is given for wave energy periods larger than 10.75 s, with a max difference of 2.17 MWh. Overall, using the Bretschneider spectrum, the AEP is 301.1 MWh (the sum of all bins in Fig. 15) less than that using the JONSWAP spectrum.

2) Bretschneider and Measured Spectra: The difference in the power production estimation using the Bretschneider spectrum when compared to the measured wave spectrum can be seen in Fig. 16. For both short wave energy periods (shorter than 7.75 s) and long wave energy periods (longer than 10.75 s), using the Bretschneider spectrum slightly under-estimates the wave energy production (the max difference is 1.72 MWh), but between 7.75 and 10.75 s, the Bretschneider spectrum may slightly over-estimate the power conversion by 4.407 MWh. Overall, using the Bretchneider spectrum under-predicts the AEP by 22.3 MWh.

3) JONSWAP and Measured Spectra: The difference in the power production estimation using the JONSWAP spectrum when compared to the measured wave spectrum is shown in Fig. 17. For short wave energy periods (shorter than 10.25 s), using the JONSWAP spectrum over-estimates the wave energy production (the max difference is 22.15 MWh), but for the wave energy periods larger than 10.75 s, the JONSWAP spectrum slightly under-estimates the power conversion by a 2.46 MWh. Overall, using the JONSWAP spectrum leads to an over-prediction in the AEP of 279 MWh (the sum of all bins in Fig. 15).

VI. Conclusion

The investigation has shown the effects of different wave spectra on the wave energy conversion assessment. The examined wave spectra include the most used theoretical wave spectra: Bretschneider, the standard JONSWAP, and the measured wave spectra. From the study, following conclusions can be drawn.

1) The overall average of the measured wave spectrum is very similar to the Bretschneider spectrum (see Fig. 7). This is a good indicator of what theoretical spectrum should be used for overall assessment for a wave energy converter. In the cases of most happened sea states (by bin) or the most energetic sea state (by bin), the average spectra are very close to the Bretschneider spectrum, although the slight differences in the peakness factor from the unit may be found ($\gamma = 1.14$ and $\gamma = 1.25$, respectively).
2) Using different theoretical spectra (i.e., the most popular ones: Bretschneider and JONSWAP), the assessment of the wave energy production can vary significantly. For the individual sea state, the max difference can be up to 40%, whereas difference for the AEP can be 18.1% (JONSWAP over the Bretshneider).
3) When comparing the wave energy assessments using the measured wave spectrum, the max difference for the JONSWAP spectrum is 38.8%, whereas the max difference for the Bretshneider spectrum is –7.5% (an under-prediction).
4) The AEP is over-predicted by 16.4% when using JONSWAP spectrum, and under-predicted by 1.3% when using the Bretschneider spectrum. In this case, the Bretschneider is a more accurate choice in assessing the wave energy power performance. The AEP result agrees very much with the overall measured wave spectrum, which is much closer to the Bretshneider spectrum.

References

[1] EC, "A European strategic energy technology plan (SET-Plan): Towards a low carbon future," COM(2007) 723 Final 2007, 2007. [Online]. Available: http://eur-lex.europa.eu/legal-content/EN/TXT/PDF/?uri=CELEX:52007DC0723&from=EN. Accessed on: Jun. 9, 2017.

[2] OEE, Europe Needs Ocean Energy, 2016. [Online]. Available: https://www.oceanenergy-europe.eu/en/communication/why-ocean-energy. Accessed on: Jun. 1, 2017.

[3] D. Magagna and A. Uihleih, "Ocean energy development in Europe: current status and future perspectives," *Int. J. Mar. Energy*, vol. 11, pp. 84–104, 2015. doi: 10.1016/j.ijome.2015.05.001.

[4] OpenHydro, OpenHydro: Tidal Technology. [Online]. Available: http://www.openhydro.com/company.html. Accessed on: Oct. 15, 2017.

[5] OceanEnergy, Ocean Energy: A World of Power, 2017. [Online]. Available: http://www.oceanenergy.ie/. Accessed on: Oct. 15, 2017.

[6] SeaPower, The Sea Power Platform, 2015. [Online]. Available: http://www.seapower.ie/. Accessed on: Mar. 5, 2015.

[7] ESBi, Accessible Wave Energy Resource Atlas: Ireland, 2005. [Online]. Available: https://www.marine.ie/Home/sites/default/files/MIFiles/Docs/General/waveatlas.pdf

[8] T. Heath, "A review of oscillating water columns," *Philos. Trans. Roy. Soc. A, Math., Phys. Eng. Sci.*, vol. 370, pp. 235–245, 2012. doi: 10.1098/rsta.2011.0164.

[9] R. Yemm *et al.*, "Pelamis: Experience from concept to connection," *Philos. Trans. Roy. Soc. A, Math., Phys. Eng. Sci.*, vol. 370, pp. 365–380, 2012.

[10] A. Henry *et al.*, "Advances in the design of the Oyster wave energy converter," in *Proc. Royal Inst. Naval Architect's Mar. Offshore Renewable Energy Conf.*, London, U.K., Apr. 2010, pp 21–23.

[11] OPT, Ocean Power Technology, 2015. [Online]. Available: http://www.oceanpowertechnologies.com/. Accessed on: Mar. 5, 2015.

[12] Wave Dragon, 2017. [Online]. Available: http://wavedragon.net/index.php?option=com_content&task=view&id=6. Accessed on: Oct. 25, 2017.

[13] WaveStar, 2017. [Online]. Available: http://wavestarenergy.com/. Accessed on: Oct. 25, 2017.

[14] CorPower, CorPower: Resonant Wave Power, 2017. [Online]. Available: http://www.corpowerocean.com/. Accessed on: Oct. 25, 2017.

[15] FPP, Floating Power Plant, 2017. [Online]. Available: http://www.floatingpowerplant.com/products/. Accessed on: Jun. 10, 2017.

[16] Y. H. Yu *et al.*, "Experimental wave tank test for reference model 3 floating-point absorber wave energy converter project," Nat. Renewable Energy Lab., Golden, CO, USA, Tech. Rep. NREL/TP-5000-62951, 2015.

[17] W. Sheng and A. Lewis, "Power takeoff optimisation for maximising energy conversion of wave-activated bodies," *IEEE J. Ocean. Eng.*, vol. 41, no. 3, pp. 529–540, Jul. 2016, doi: 10.1109/JOE.2015.2489798.

[18] RMP, Reference Model Project (RMP), 2014. [Online]. Available: http://energy.sandia.gov/energy/renewable-energy/water-power/technology-development/reference-model-project-rmp/. Accessed on: Apr. 4, 2018.

[19] V. S. Neary *et al.*, "Methodology for design and economic analysis of marine energy conversion (MEC) technologies," Sandia Nat. Lab., Albuquerque, NM, USA, Tech. Rep. SAND2014-9040, 2014.

[20] W. Sheng and A. Lewis, Wave energy converters: Fix- or self-referenced? in *Progress in Renewable Energies Offshore*, C. G. Soares, Ed. Lisbon, Portugal: CRC Press, 2016, pp. 255–262.

[21] B. G. Cahill and A. Lewis, "Wave energy resource characteristion of the Altantic marine energy test site," *Int. J. Mar. Energy*, vol. 1, pp. 3–15, 2013. doi: 10.1016/j.ijome.2013.05.001.

[22] A. Falcao, "Phase control through load control of oscillting-body wave energy converters with hydraulic PTO system," *Ocean Eng.*, vol. 35, pp. 358–366, 2008. doi: 10.1016/j.oceaneng.2007.10.005.

[23] DNV, *Environmental Conditions and Environmental Loads*, 2010. [Online] Available: https://rules.dnvgl.com/docs/pdf/DNV/codes/docs/2010-10/RP-C205.pdf. Accessed on: Mar. 31, 2017.

[24] M. J. Tucker and E. G. Pitt, *Waves in Ocean Engineering*. Oxford, U.K.: Elsevier, 2001.

James Prendergast received the B.Eng. degree in energy systems engineering with civil from the National University of Ireland Galway, Galway, Ireland, in 2016, and the M.Eng.Sc. degree in sustainable energy from the University College Cork, Cork, Ireland, in 2017.

In 2017, he joined the Electricity Supply Board, Ireland's leading energy utility, where he is currently an Engineer in the engineering arm of the company.

Mingfang Li received the B.S. and Ph.D. degrees from Wuhan University, Wuhan, China, both in mechanical engineering and structural engineering.

He is a Lecturer with the Wuhan University of Science and Technology. He is currently a Visiting Scholar with the Centre for Marine and Renewable Energy Ireland, Environmental Research Institute, University College Cork, Cork, Ireland. His research work is mainly on the device and technology development for marine renewable energy conversion and also in active control and numerical simulation.

Wanan Sheng received the B.Sc. degree in physics from Jiangxi Normal University, Nanchang, China, in 1985, the M.Sc. degree in marine hydrodynamics from the Naval Academy of China, China, in 1990, and the Ph.D. degree in aerospace engineering from the University of Glasgow, Glasgow, U.K., in 2004.

He is currently a Senior Research Fellow and the Lead Hydrodynamicist with the Centre for Marine and Renewable Energy Ireland, Environmental Research Institute, University College Cork, Cork, Ireland. His research work is mainly on the device and technology development for marine renewable energy conversion, and his research on the fundamental problems in wave energy conversions and on the cost reduction of wave energy production has led to fruitful publications and technology improvements. He has authored or coauthored 40 peer-reviewed journal papers and 38 peer review conference papers, together with 4 book chapters. He also worked on unsteady aerodynamics for helicopters and wind turbines and proposed a semiempirical dynamic stall model, which is now being used in the aerodynamics of helicopters, wind, and tidal turbines.